Science
AAAS

Supplementary Materials for

Functional diversification of a wild potato immune receptor at its center of origin

Yerisf C. Torres Ascurra *et al*.

Corresponding authors: Thorsten Nürnberger, nuernberger@uni-tuebingen.de; Vivianne G. A. A. Vleeshouwers, vivianne.vleeshouwers@wur.nl

Science **381**, 891 (2023)
DOI: 10.1126/science.adg5261

The PDF file includes:

Other Supplementary Material for this manuscript includes the following:

Materials and Methods

Plant material

Potato plants were maintained and clonally propagated in vitro on MS medium (*49*) supplemented with 20% sucrose at 25 °C. For experiments, 2 weeks old plantlets were transferred to sterilized soil and grown in regulated greenhouse compartments at 18-22 °C, 16h/8h day/night regime and 70% relative humidity. *Nicotiana benthamiana* plants were generated from seeds and grown under the same greenhouse conditions.

Peptides and protein

Peptides were synthesized by Genscript USA Inc, prepared as 1 mM stock solutions in (DMSO), and diluted in MilliQ water or sterile tap water before use. INF1 was produced as described previously (*50*).

Peptide infiltrations

Peptides were infiltrated at 1 μM concentrations into the abaxial side of leaves of at least 3 plants per genotype (three leaves per plant were used), using needleless syringes. The cell death intensity was scored 3-4 days after infiltration as previously described (*51*). A scale from 0 to 1 was used, based on the cell death percentage of the infiltrated area. 0 indicates no symptoms, 1 indicates confluent cell death and intermediate values were also considered for chlorosis or increasing levels of patchy cell death. Average scores ≤ 0.2 were considered as non-responsive and excluded from further analysis. The classification of potato genotypes into classes 1-5 is based on their ability to develop cell death after treatment with Pep-25 and the mutant peptides Pep-25W231A, Pep-25P234A and P-25Y241A.

Genetic mapping of *PERU*

An F1 population (named 3240) was generated by crossing the double monoploid *Solanum tuberosum* group Phureja DM 1-3 516 R44 as female parent with the diploid *Solanum tuberosum* RH89-039-16 as male parent. To generate a segregating population, one individual from F1 (3240-4) was backcrossed with RH89-039-16. To confirm the previous mapping of the receptor a small set of the population (30 individuals) and the parents were genotyped with 20 molecular markers. For the fine-mapping a high-throughput recombinant screening was followed (*52*). Briefly, seeds were sown in vitro, the emerging seedlings were transferred to new pots containing MS20 medium. DNA of the individual seedlings was isolated and genotyped with two flanking markers. The recombinant plants were transferred to the greenhouse and phenotyped for Pep-13-induced cell death. This process was iterated until a small mapping interval was obtained. Molecular markers like HRM (High resolution melting), CAPS (Cleaved amplified polymorphic sequence) and PCR-

absence/presence were developed based on DM genome sequence *(14)*. In the first round of fine-mapping 12 markers spanning 1.3 Mb of the top of chromosome 3 were used and 1,918 plants were genotyped, and in the second round of fine-mapping, additional 15 markers were developed to genotype 289 plants. The primers used to genotype the plants are listed in table S2.

Cloning of candidate genes and homologs

Leaves from DM and Pep-25-responding wild *Solanum* spp. were infiltrated with 1 μM Pep-25 and harvested after 5 hours. RNA was isolated using the RNeasy Plant Mini Kit (Qiagen) and converted to cDNA using the Maxima H minus reverse transcriptase kit (Thermo Scientific). Specific primers (table S2) were designed and sequences encoding candidate Pep-13 receptors were cloned into pENTR™/D-TOPO® vector and then transferred to the destination vector pK7WG2, under 35S promoter.

Transient expression of Pep-13 receptor candidate-encoding genes in *N. benthamiana*.

Cells of *Agrobacterium tumefaciens* strain AGL1 were transformed with Pep-13 receptor candidate-encoding gene constructs and agroinfiltration assays were performed as described *(21)*. Leaf infiltration with Pep-13 with GP42 were performed 2 days upon infections with *A. tumefaciens*. Three days after the peptide infiltration, the leaves were scanned in a ChemiDoc MP imaging system, model Universal Hood III (Bio-Rad), and cell death images were acquired with filters capturing the light emitted in the red visible spectrum (filter 605/50) *(46)*.

Stable transformation of potato cultivar Atlantic

Stable transformation of potato cultivar Atlantic with a *35S*::*PERU* construct in plasmid pK7WG2 was carried out using routine potato transformation protocols (*53*). Fourteen independent transgenic lines were tested for the presence of *PERU*-encoding sequences using gene-specific primers. All but one line tested positive and responded to Pep-13. Lines *PERU*#10 and *PERU*#11 were selected for further experiments.

Ethylene production

Leaves of 4-week old potato plants were cut in round pieces (6.0 mm diameter) and floated in MilliQ water overnight. Four leaf pieces were incubated in sealed 10 ml vials containing 0.6 mL 20mM MES buffer, pH5.7 and the indicated elicitor. Ethylene accumulation was measured after 4 hours of incubation by gas chromatographic analysis (TraceGC1300 (InterScience, Breda, NL) coupled with a flame ionization detector (FID, Temperature = 260°C, cycle time = 3 min, columns: Agilent J&W GS-GasPro 10m 0.32 mm ID coupled with Agilent J&W GS-GasPro 20m 0.32 mm ID to assure backflush, injection volume: 250 μL)) of 3.5 mL of the air drawn from the closed vial with a syringe. At least three measurements were performed for each treatment.

ROS production

Leaves of 4-week-old potato plants were cut in round pieces (6.0 mm diameter), placed in 96 well white plate containing 50 µL of MilliQ water, and incubated overnight. Water was removed and replaced with 50 µL of fresh MilliQ water. After that, 50 µL of a solution containing 10 µg horseradish peroxidase, 50 µM luminol L-012, and elicitor was added. Luminescence was determined using a CLARIOstar plate reader (BMG LABTECH) over a period of 3 hours.

Generation of *PERU* knockout DM plants

Golden Gate cloning was used to generate the constructs as described previously (*54, 55*). Four sgRNAs that target the LRR domain were designed using CRISPOR (http://crispor.tefor.net/), and synthesized as sense and antisense primers (Biolegio BV, The Netherlands). The four sgRNAs were fused to U6-26 promoter and terminator from *Arabidopsis thaliana*, and cloned into the level 1 acceptors pICH47761, pICH47772, pICH47781, and pICH4491 respectively. Then, they were assembled into the Level 2 acceptor pICSL4723 together with NPTII, Cas9 and turbo RFP. Stable transformation of DM 1-3 516 R44 was performed using routine potato transformation protocols (*53*). Gene-specific primers (CC-238-fw & CC-1440-rv and CC-4225-fw & CC-5129-rv) were used to amplify and sequence *PERU* fragments of the transformants. CC-238-fw & CC-1440-rv product showed the occurrence of 2 deletions (15 and 72 bp) and 1 big deletion (418 bp) in the CRISPR lines *peru* #29 and #32 respectively. Pep-13 infiltrations and ROS assays were performed to confirm the phenotype. The primers used for cloning the gRNAs and for genotyping the transformants are listed in table S2.

Virus-induced gene silencing assays

Cotyledons of 2 week-old tobacco seedlings were infiltrated with 1:1 mixtures of pTRV1 and pTRV2::*NbSERK3,* pTRV2::*NbSOBIR1/-like*, pTRV2::*PDS*, or pTRV2::*GUS*, at a final OD_{600} of 1.0. TRV:PDS and TRV:GUS were used as controls. After two weeks, Pep-13 or INF1 protein were infiltrated, and the leaves were scanned in a ChemiDoc MP imaging system (Universal Hood III, Bio-Rad) and cell death images were acquired with filters capturing the light emitted in the red visible spectrum (filter 605/50) (*56*).

Quantitative reverse-transcription PCR

Leaf discs were sampled and stored at -80 °C. RNA isolation was performed using RNeasy Plant Mini Kit (Qiagen) and following the manufacturer instructions. The iScript™ cDNA Synthesis Kit (Bio-rad) and iScript Reverse transcription supermix (Bio-rad) were used for cDNA synthesis and RT-qPCR. *NbUbe35* and *NbNQO* were used as reference genes (*57*).

Phytophthora infestans infection assay

Disease tests were performed on whole plants as previously described *(27)*. The *P. infestans* isolate Dinteloord was grown at 18 °C in the dark on rye agar medium (*58*) supplemented with 20g/L sucrose. To obtain zoospores, the mycelium was flooded with cold water (4 °C), the suspension was transferred to a new tube and incubated at 4 °C for 2 hours. The number of zoospores was counted and adjusted to $5x10^4$ zoospores/mL for inoculation. Intact, four weeks-old potato plants were spot-inoculated with zoospore suspensions. Lesion diameters were measured at 3, 4 and 5 dpi.

In vivo cross-linking and immunoprecipitation assays

A. tumefaciens (strain GV3101) harboring the corresponding constructs were grown in LB medium with appropriate antibiotics at 28 °C overnight, harvested and resuspended in 10 mM $MgCl_2$, 10 mM MES pH 5.7, 200 µM acetosyringone to desired OD_{600}. The cultures carrying appropriate constructs were mixed to final OD_{600} = 0.1 $construct^{-1}$, incubated at room temperature for 1-2 hours, and infiltrated into 5-6-week-old *N. benthamiana* plants. Leaves were harvested 48 hours after infiltration of bacteria for the following assays.

For in vivo cross-linking, leaves of *N. benthamiana* expressing PERU-GFP were infiltrated with Pep-25-bio or Pep-25W231A-bio with or without unlabeled Pep-13 or Pep-13W231A peptides as competitor. For cross-linking of peptides to the receptor, 2 mM ethylene glycol bis (succinimidyl succinate) (EGS) was co-infiltrated into the leaves. After 20 minutes, the leaves were harvested and frozen in liquid nitrogen. For immunoprecipitations, membrane proteins of infiltrated *N. benthamiana* leaves were extracted using extraction buffer (150 mM NaCl, 50 mM Tris·HCl pH 8.0, 1% NP-40, protease inhibitor cocktail (RoChe)), adjusted to a final concentration of 1 mg ml^{-1} and immuno-adsorbed by means of their GFP-tags on GFP-Trap agarose beads (ChromoTek). Immunoblots were developed either directly with Streptavidin-alkaline phosphatase conjugate (Roche), with anti-GFP antibodies (Torrey Pines Biolabs) or anti-myc antibodies (Sigma-Aldrich), followed by staining with secondary antibodies coupled to alkaline phosphatase and CDP-Star (Roche) as substrates.

Protein expression and purification in insect cells

The sequence encoding ectodomain of $PERU^{24-779}$ with an N-terminal gp67 secretion signal peptide was amplified by nested PCR and cloned into pOET1C transfer vector (*Apa*I-*Sac*II sites) with C-terminal 6xHis-fusion (Oxford Expression Technologies). The resulting plasmids were transfected into Sf9 cells by using flashBAC GOLD kit (Oxford Expression Technologies). High Five cells (Invitrogen) were infected with 3% (vol/vol) virus at a density of $1x10^6$ cells ml^{-1} and incubated at 27 °C for 48 hours. The secreted proteins were purified from the supernatant by a HisTrap excel column (GE Healthcare). Bound proteins were eluted in a buffer containing 50 mM

Tris·HCl pH 8.0, 200 mM NaCl, 500 mM imidazole and further purified by size-exclusion chromatography (Superdex 200 Increase 10/300, GE Healthcare) in a buffer containing 20 mM NaAc pH 5.0, 200 mM NaCl.

In vitro ligand binding assays

The purified His_6-tagged PERU LRR ectodomain protein ($PERU^{LRR}$-His_6) was mixed with 2 mM EGS and Pep-25-bio, with or without unlabeled Pep-13 peptide in binding buffer (20 mM NaAc pH 5.0, 200 mM NaCl). After incubation at room temperature for 30 minutes, streptavidin agarose resin (Thermo Scientific) was added and further incubated on a rotor at 4 °C for 1 hour. The resin was washed with binding buffer for 3 times. $PERU^{LRR}$-His_6 bound Pep-25-bio peptides were detected by immunoblots as described above. The band intensities of streptavidin were measured using ImageJ.

Phylogenomic analyses

A database of 6,630,292 protein sequences was assembled from 124 Solanaceae genomes (data S4). Receptor kinases (RKs) were then extracted from the compiled protein dataset using hmmsearch (HMMER v3.3.2) [--max], utilizing the PF00069 Pfam HMM profile, with only sequences bearing a single protein kinase (PK) domain retained (*59*). These RK sequences were then subjected to a search for leucine-rich repeat (LRR) domains using the Pfam PF00560, PF13855, PF08263, and PF13516 HMM profiles, with sequences identified by any of these profiles considered to possess an LRR domain. The PK domain sequences were then extracted using the domain boundaries within the domain table output from hmmsearch for alignment and phylogenetic analysis. A phylogenetic tree was constructed using MAFFT v7.520 [--anysymbol] and FastTree v2.1.11 [default options], involving 42,697 sequences from the previous step and 33 reference sequences, including $PERU^{DM}$. LRR-RK subgroups were annotated based on their representatives (data S7, S8) (*60, 61*).

LRR-RK Subgroup XII, which contained FLS2 and $PERU^{DM}$, was extracted and the PK domains were realigned to generate a new phylogenetic tree (data S9). Major branches close to $PERU^{DM}$ and FLS2 were identified and extracted. While FLS2 clade was easy to identify, $PERU^{DM}$ clade required multiple iterations of zooming, filtering, and realignment to improve resolution and identify the best branch defining the $PERU^{DM}$ clade. Sequences with potential truncated PK domains were excluded using Geneious prime software (https://www.geneious.com/), based on the length distribution graph.

$PERU^{DM}$ and FLS2 clades were then subjected to additional refining steps: the N-terminally truncated sequences without the LRRNT cap (PF08263) were removed, as were sequences with additional domains to PK and LRR. Sequences with incorrect gene models were trimmed, specifically those with incorrect start codons (N-terminal extension). PERU sequences were

checked to determine whether the first intron was miscalled in the alignment. Lastly, sequences without a signal peptide, as determined by SignalP 6.0, were filtered out (*62*). Next, potentially truncated FLS2 sequences were removed by setting a length threshold of 1150 amino acids and over based on FLS2 clade sequence length distribution (data S5, S10). Finally, the full-length sequences of refined PERU^{DM} and FLS2 clades were used to make the final phylogenetic trees in the same way as described before. The phylogenetic trees were visualized by iTOL and annotated manually (*63*). The species tree was adapted from *(47).* All datasets, scripts and instructions for these analyses are available in the GitHub repository on Zenodo *(48)*.

Positive selection analysis

36 full-length nucleotide sequences were used, that form the PERU clade (Fig. 4A), to generate a codon alignment using MUSCLE from MEGA software package (*64*). To identify which PERU amino acids have been affected by diversifying selection, we used maximum likelihood models of codon substitution. Analyses were performed with the program CODEML from the PAML package *(34)*. The six models recommended were tested (Null models M0, M1, M7 and alternative models M3, M2, M8, respectively) Statistical significance was tested by comparing the null models with their respective alternative models. Twice the difference in log likelihood ratio between a null model and an alternative model was compared with a chi-squared (χ^2) distribution. The degrees of freedom were determined by the difference in the numbers of parameters estimated from the pair of models. The likelihood ratios of the two models test whether an alternative model fits the data better than the null model. Positively selected sites were identified using the Bayes Empirical Bayes analysis implemented in CODEML (*65*).

Structural analysis using AlphaFold2 and LRR prediction

The ectodomain of PERU^{DM} (PERU^{DM}-ECD) which comprises residues 39-768 was modelled using AlphaFold2 (AF2) through ColabFold v1.5.2 (*66, 67*), following guidelines on the document (https://colab.research.google.com/github/sokrypton/ColabFold/blob/main/batch/AlphaFold2_batch.ipynb). Twelve iterative recycles and an AMBER relaxation step were incorporated in the modelling. From the 5 independent models generated by AF2, we selected the highest-ranking model based on the average per-residue confidence metric, pLDDT. The number of LRRs were checked manually and confirmed by AF2.

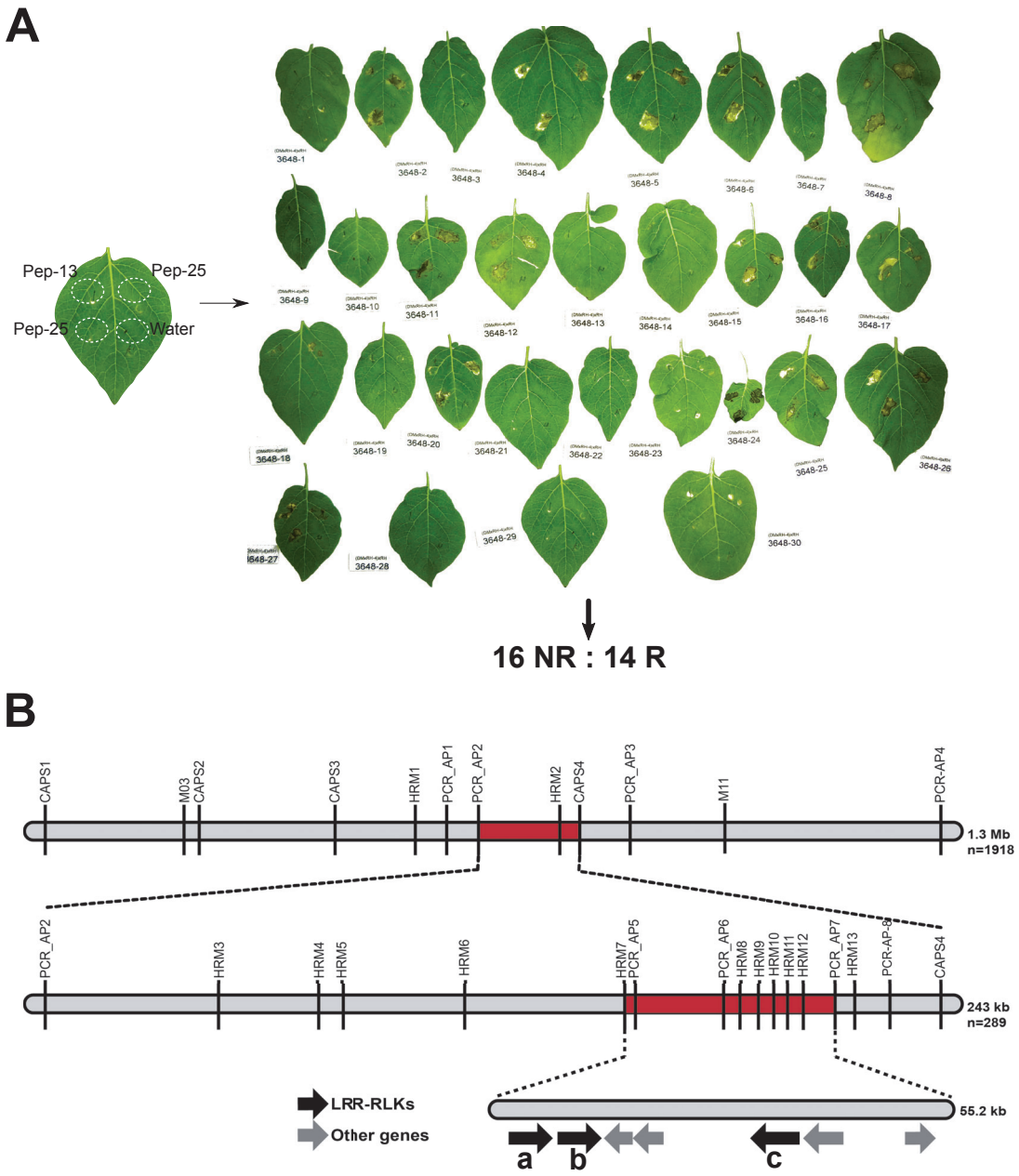

Fig. S1. Map-based cloning of *PERU* from DM 1-3 516 R44. (A) The F2 segregating population 3648 was phenotyped for a cell death response (R, responsive; NR, non-responsive) to Pep-13/25 and segregated in a 1:1 ratio. **(B)** Two flanking markers PCR_AP2 and CAPS4 were identified after the high throughput screening of 1918 individuals from the mapping population, narrowing the mapping interval to 243 kb. To further fine-map the region, 15 molecular markers were developed and 289 additional individuals were genotyped to find new recombination events. As a

result, a final mapping interval of 55.2 kb was obtained, which contains 7 genes, 3 of which (“a”, “b” and “c”) encode LRR-RKs. Other genes (grey arrows, from left to right) include sequences encoding SOS3-interacting protein, seed dormancy control domain containing protein, neutral/alkaline non-lysosomal ceramidase and homeodomain-like superfamily protein.

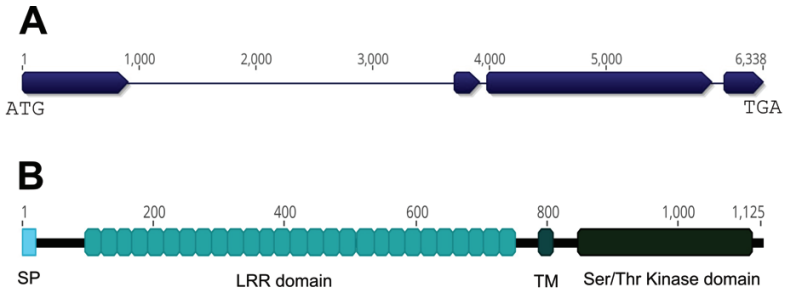

C

	1
Signal peptide	MEKAFTFFLLTILLLLHYVMT
	2
N-terminus	QTNITTDQLALLSLKSQISSDPFHY
	LNESWSPAINVCRWVGVTCGSRHQR
	VKSLNLSDMTLTGTIPRDLGNLTF
	97
LRR domain	LISLDLGSNNFHGNLPQEIARLSR
	LKFLDLSFNKFRGEIPSWFGFLER
	LQVLNLRSNSFTGFIPPSLSNASR
	LETLEISANLLEGNIPEEIGNLHN
	LNLLSIQHNKLTGSIPFTIFNISS
	IEVIAFTNNSLSGNLPNGLCNGLPI
	LKELRLSVNKLHGHMPKSLSNCSQ
	LQKLSLSGNDFDGPIHSEIGRLSN
	LQILYLGANHFTGIIPQEIGNLVN
	LMKLAVEINQITSSIPISIFNISS
	LQEVSLWKNNLKGSLPREIGNLTK
	MQFLYLEENRFTGEIPKEIRNLVE
	LEELNLELNSFSGSLPMEIFNISR
	LRIMSLSANNLSGTLPPNIGSTLPN
	IEELYLHGLTNLVGTIPHSISNCSK
	LNNLELSQNKLTGLIPNSLGYLTH
	LHYLNLQRNNLTSDSFLSFLTSLTNCRN
	LTSLYLSFNPLNAMLPVSVGNFSKS
	LIKFDANACNIKGKIPNEVGNLSN
	LLDLDLSDNNLIGSIPTSIHNMRS
	LQRLDLRNNKLTGFIGDNLCKLQH
	LGDIYLGQNQLSGALPNCLGNITS
	LRFLHLDSNKLSSNIPTSLGNLKD
	LIKLHLSSNNMVGSLPPEIGGLQN
	LVHLSLRHNKLQGSIPDSVSNMVG
	LEFLDISHNDISGSIPMSMEKLQN
	LKYFNVSVNKLYGEIPSGGPFKNL
	752
Juxtamembrane extracellular	SSQFFIDNEALCGSSRFSVPPCAT
	SSKHRSNRKKM
	787
Transmembrane	LVLFLVLGIALVFVPITFVFLWI
	810
Juxtamembrane intracellular	RYRRGKRSPQRADSLSIATTERIS
	YYELLQATDTLGE
	847
Ser/Thr protein kinase domain	SNLIGSGSFGSVYKGVLRSGTAIA
	VKVFNLQLEAAFKSFDTECEVLRS
	LRHRNLVKVITSCSNLDFKALVLE
	YMPNGSLDKYLYSHNYFLDIRQRL
	SIMIDVACALEYLHHGCSSPVIHC
	DLKPSNVLLDEDMVAHLSDFGISK
	LLGEDESDLYTKTLATFGYIAPEY
	GLDGLVSIKCDVYSYGIMLLETFT
	RRKPTEFEGDLSLKQWVSYSLPEA
	VMDVMDANLVTPMDNRLQKELDIV
	ASIMKVALDCCAESPTRRTNMKDVV
	1112
C-terminus	GMLQKIKIQLLAC

Fig. S2. Schematic representation of *PERU* and its encoded LRR-RK. (A) Intron/exon structure of the *PERU* gene. **(B)** Schematic representation of the PERU protein consisting of 1,125 amino acid residues. **(C)** Primary structure of the PERU protein, containing a signal peptide for secretion; an extracellular LRR domain that consists of 27 repeats of the consensus sequence LXXLXLXXNXGXIPXXJGNLXX (highlighted in grey), and is flanked by two cysteine pairs (highlighted in dark grey); a single transmembrane domain; an intracellular juxta-membrane domain that contains the putative endocytosis motif YXXØ; and a Ser/Thr kinase domain.

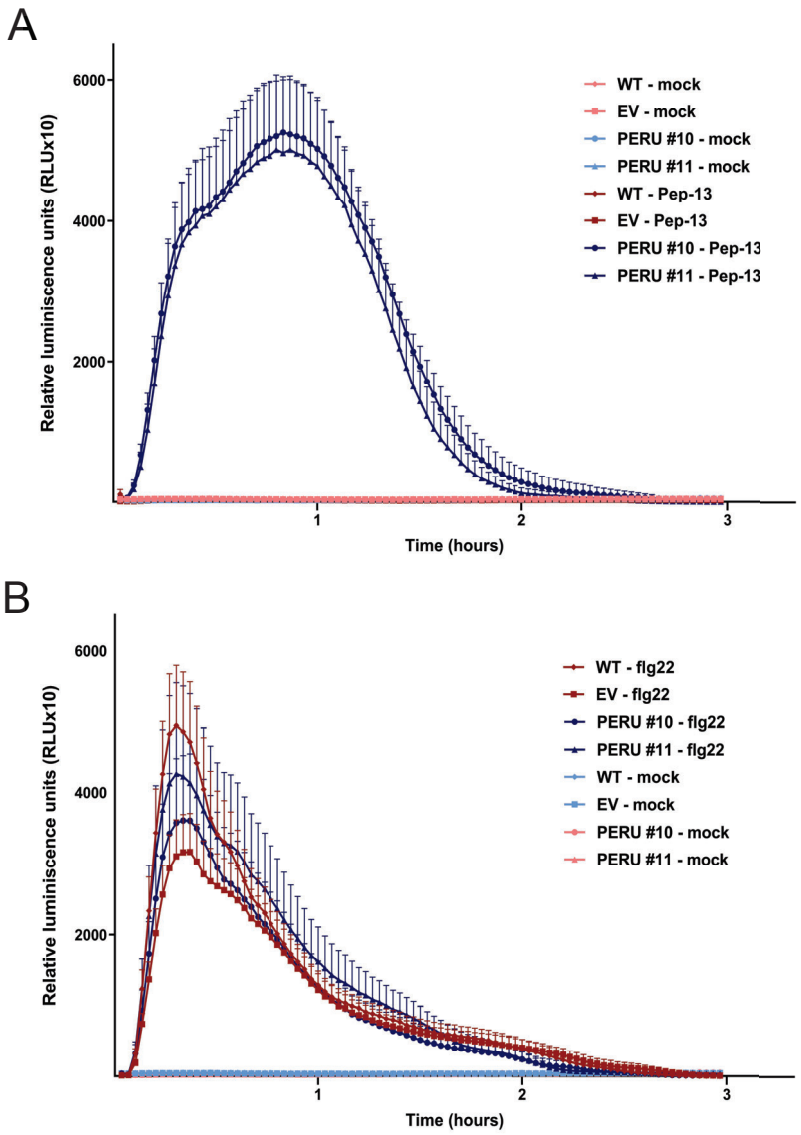

Fig. S3. ROS production in potato. Cultivar Atlantic (WT), Atlantic transformants stably expressing empty vector (EV) or *p35S::PERU* (lines #10 and #11) were treated with water (mock), or 1 µM Pep-13 **(A)** or with water, or 1 µM flg22 **(B)**. Mean values ± standard error of eight replicates are shown. Assays were performed in triplicate with similar results.

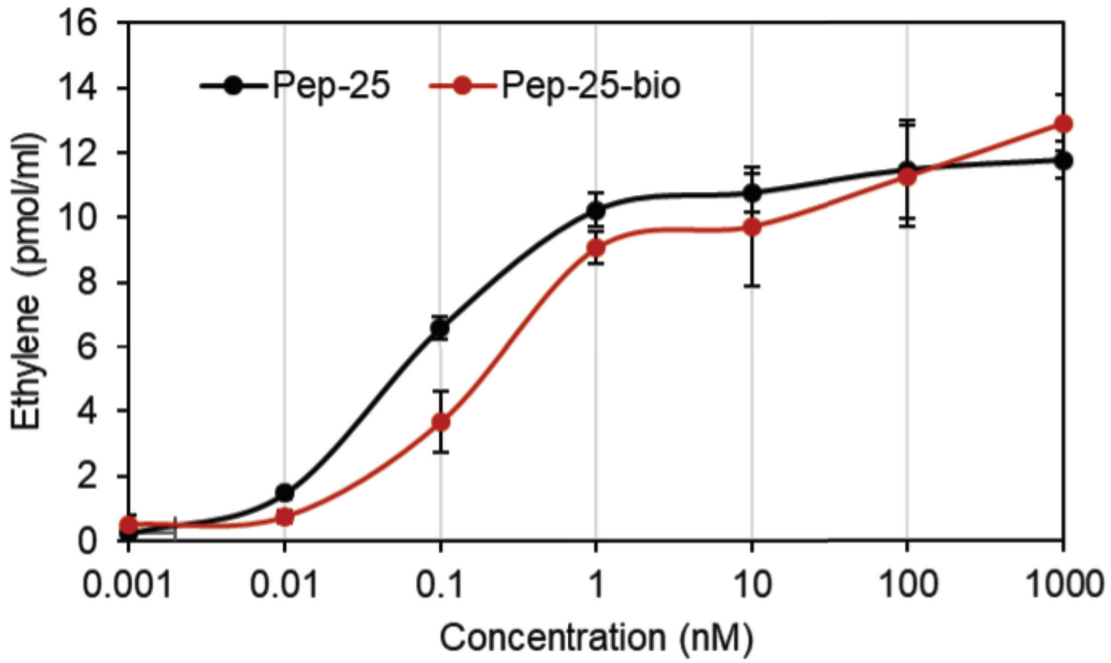

Fig. S4. Ethylene-inducing activity of biotinylated Pep-25 peptide in *N. benthamiana*. Ethylene accumulation in *N. benthamiana* leaves transiently expressing *p35S::PERU-GFP* was measured 4 hours after treatment with Pep-25 or biotinylated Pep-25 (Pep-25-bio). Bars represent means ± standard deviation of two or three replicates. Assays were performed in triplicate with similar results.

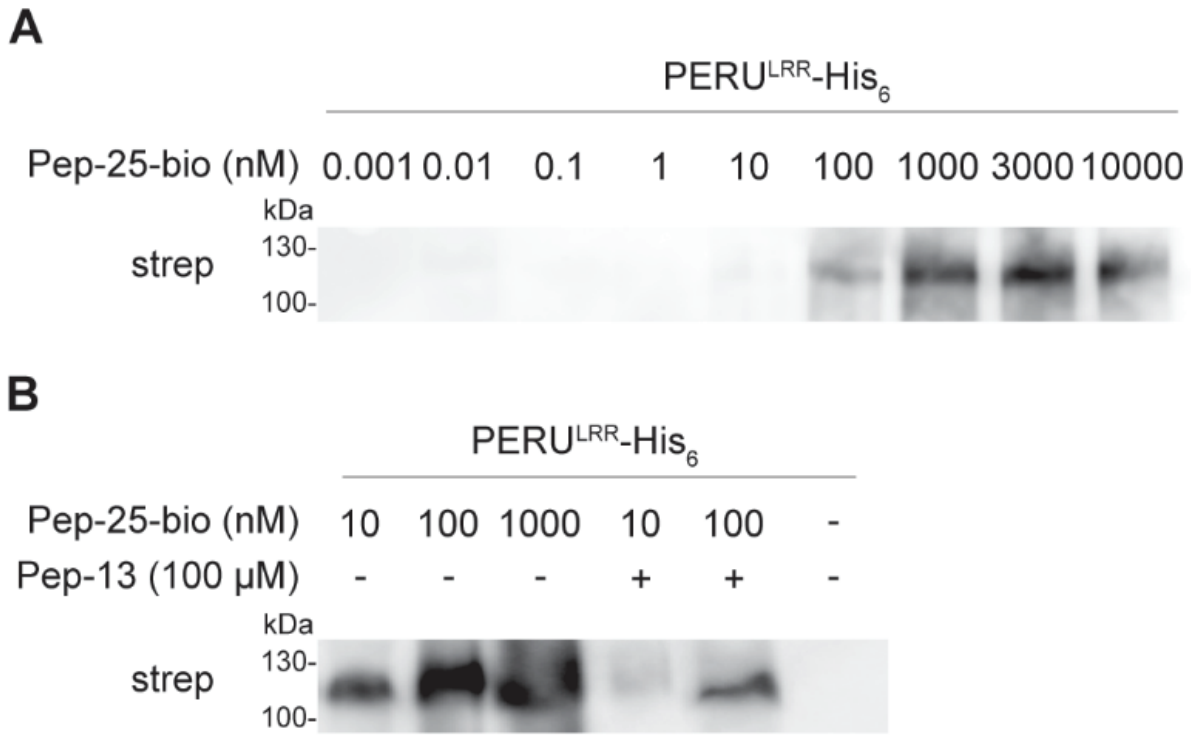

Fig. S5. In vitro binding of PERU^{LRR}-His$_6$ to Pep-25-bio. (A) Recombinant His$_6$-tagged PERU LRR ectodomain protein (PERU^{LRR}-His$_6$, 10 nM) was incubated with increasing concentrations of biotinylated Pep-25 (Pep-25-bio) as ligand. Ligand-receptor complexes were precipitated with streptavidin agarose and visualized on protein blots using Streptavidin-Alkaline Phosphatase (strep). Band intensities of strep were measured by ImageJ. The average of the affinity constants determined from five independent experiments is K_D=88.9 nM. **(B)**, Ligand binding competition experiments were conducted as in (A) using 100 µM Pep-13 as competitor. This experiment was repeated four times.

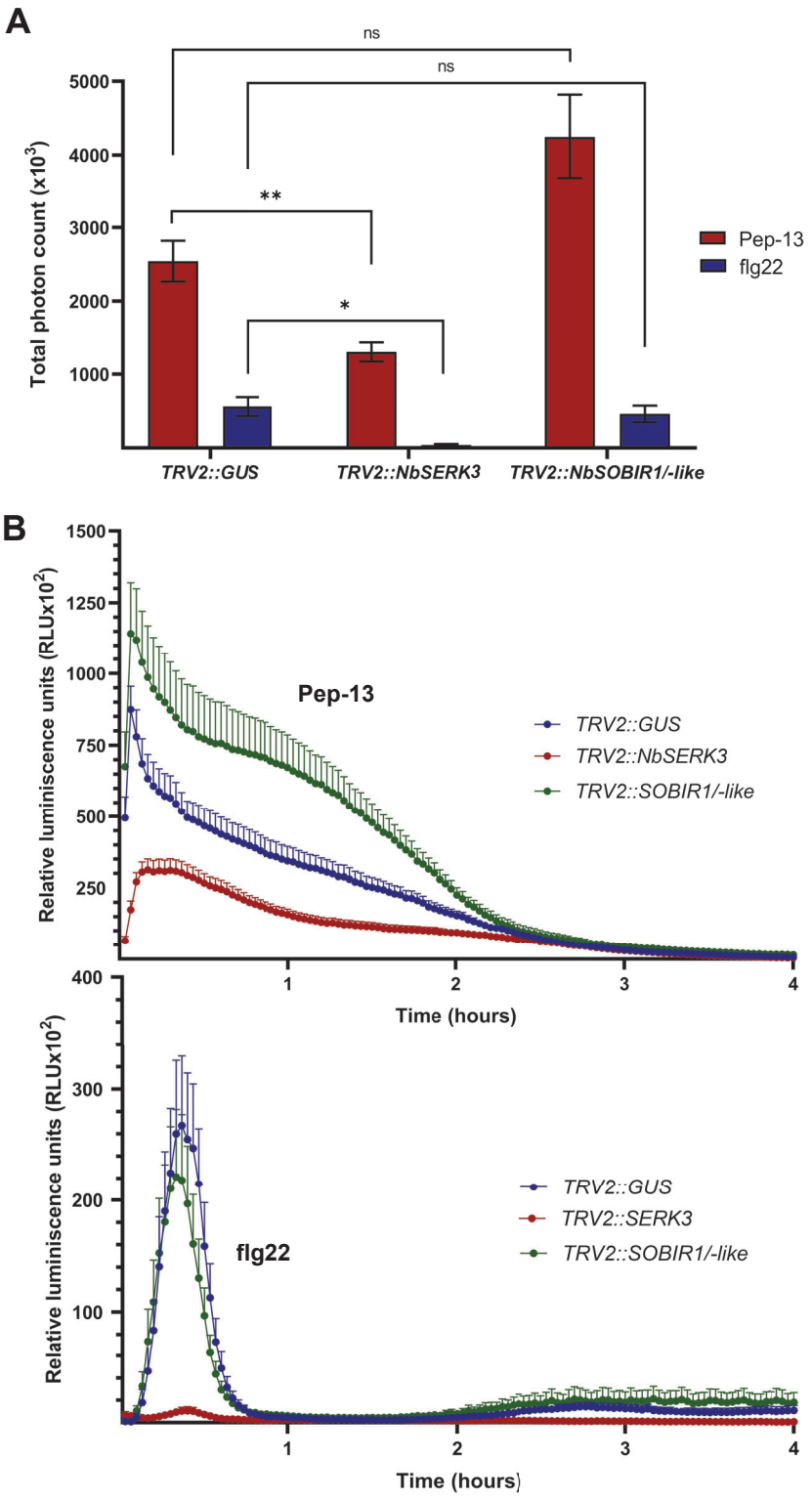
A
ns
ns
**
*
Total photon count (x10^3)
5000
4000
3000
2000
1000
Pep-13
flg22
TRV2::GUS
TRV2::NbSERK3
TRV2::NbSOBIR1/-like
B
Relative luminiscence units (RLUx10^2)
1500
1250
1000
750
500
250
Pep-13
TRV2::GUS
TRV2::NbSERK3
TRV2::SOBIR1/-like
1
2
3
4
Time (hours)
Relative luminiscence units (RLUx10^2)
400
300
200
100
flg22
TRV2::GUS
TRV2::SERK3
TRV2::SOBIR1/-like
1
2
3
4
Time (hours)

Fig. S6. Silencing of *NbSERK3* reduces the ROS burst induced by Pep-13. (A) Total photon count and **(B)** kinetics of ROS burst induced by 1 μM Pep-13 or 1 μM flg22 (as positive control) in *N. benthamiana* leaves expressing constructs *NbTRV2::NbSERK3*, *NbTRV2::NbSOBIR1/-like* or *TRV2::GUS* as control for virus-induced gene silencing. Data from (A) were analyzed using Welch ANOVA and Dunnett's T3 multiple comparison test, (*p-value 0.05, **p-value<0.01, ns non-significant). Mean values ± standard error of eight replicates are shown. Assays were performed in triplicate with similar results and representative results are shown.

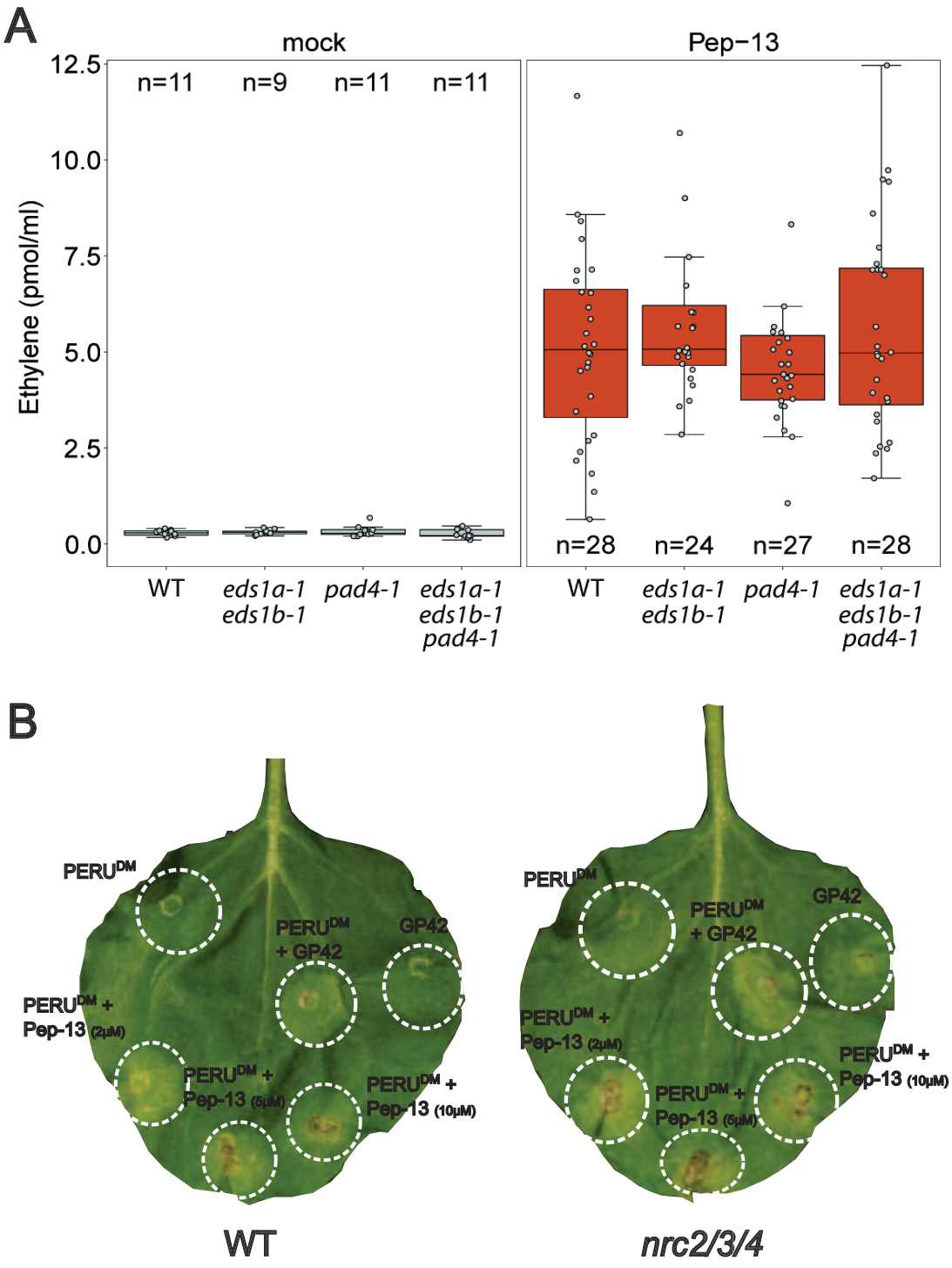
A
mock
Pep−13
Ethylene (pmol/ml)
12.5
10.0
7.5
5.0
2.5
0.0
n=11
n=9
n=11
n=11
n=28
n=24
n=27
n=28
WT
eds1a-1 eds1b-1
pad4-1
eds1a-1 eds1b-1 pad4-1
B
PERUDM
PERUDM + GP42
GP42
PERUDM + Pep-13 (2μM)
PERUDM + Pep-13 (5μM)
PERUDM + Pep-13 (10μM)
WT
nrc2/3/4

Fig S7. Pep-13-induced defenses are not impaired in *N. benthamiana* mutant genotypes transiently expressing *PERU^{DM}*. (A) Ethylene accumulation 3 hours after treatment with water (mock) or 1 μM Pep-13 in *N. benthamiana* wild-type (WT) and CRISPR mutants (eds1, pad4, and eds1/pad4) leaves transiently transformed with *PERU^{DM}-GFP*. Data points (grey dots) from three independent experiments are shown (n with exact numbers are indicated in the box plots) and plotted as box plots (center line: median, bounds of box: the first and third quartiles, whiskers: 1.5x the interquartile range, error bar: minima and maxima). **(B)** Representative WT and nrc2/3/4 mutants *N. benthamiana* leaves co-agroinfiltrated with *PERU^{DM}*, and Pep-13 (at 3 different concentrations) or the full-length glycoprotein *GP42*. Cell death was visualized at 3 days post infiltration.

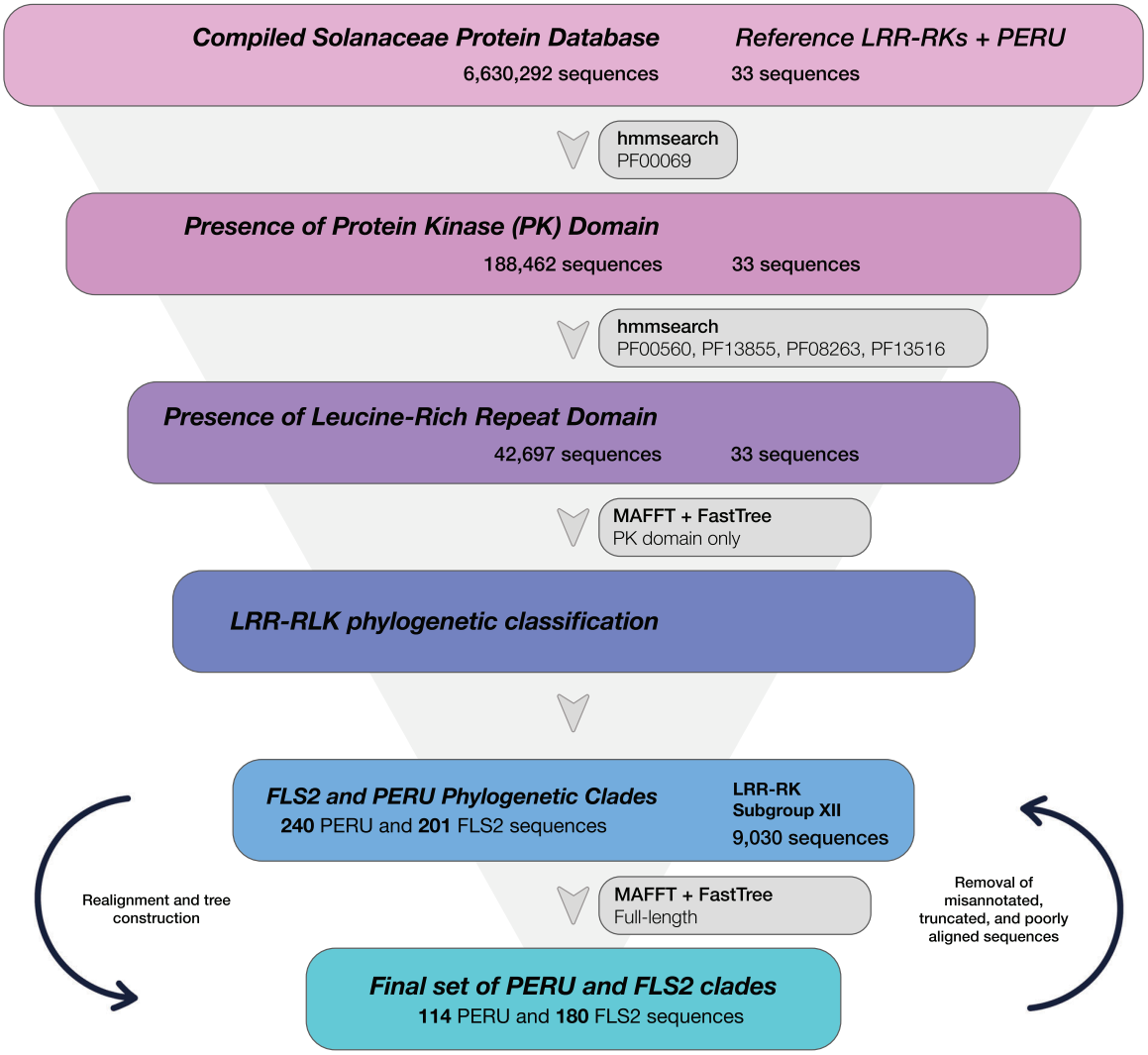

Fig S8. Bioinformatics pipeline to extract PERU and FLS2 clades. From a database containing 6,630,292 predicted sequences from 124 Solanaceae genomes, 42,697 LRR-RK proteins were obtained (table S4). These proteins were categorized based on known LRR-RK subgroups. FLS2 and PERU sequences from subgroup XII were then extracted and iteratively refined. Phylogenetic analyses were ultimately conducted using a final selection of 114 PERU and 180 FLS2 sequences.

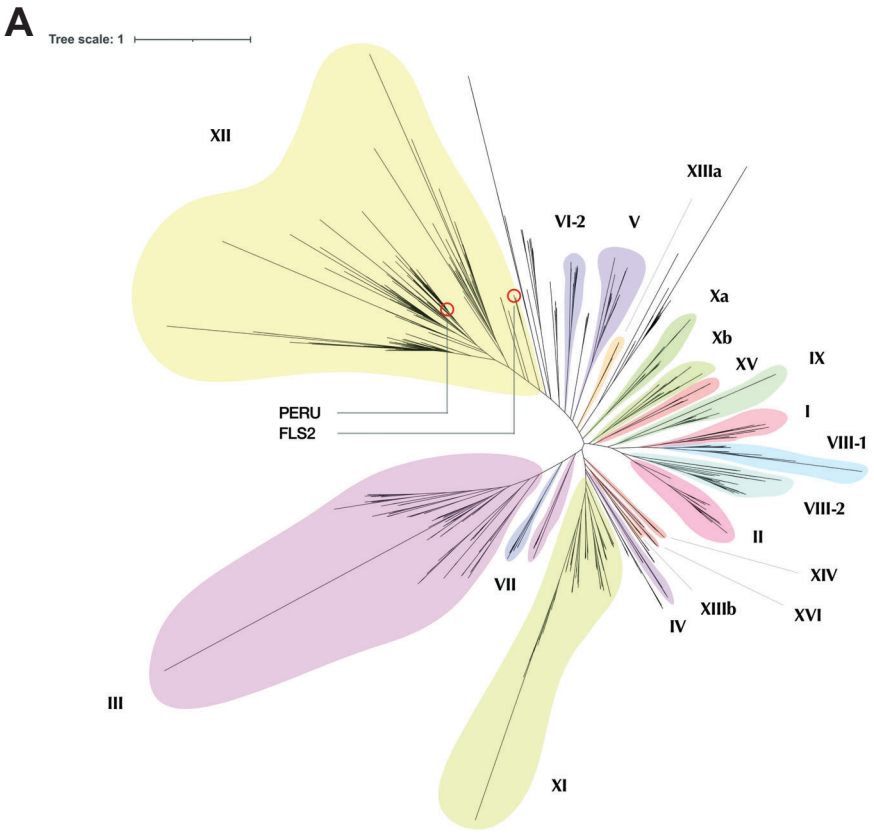
A
Tree scale: 1
XII
XIIIa
VI-2
V
Xa
Xb
XV
IX
I
VIII-1
VIII-2
II
XIV
XVI
XIIIb
IV
VII
III
XI
PERU
FLS2

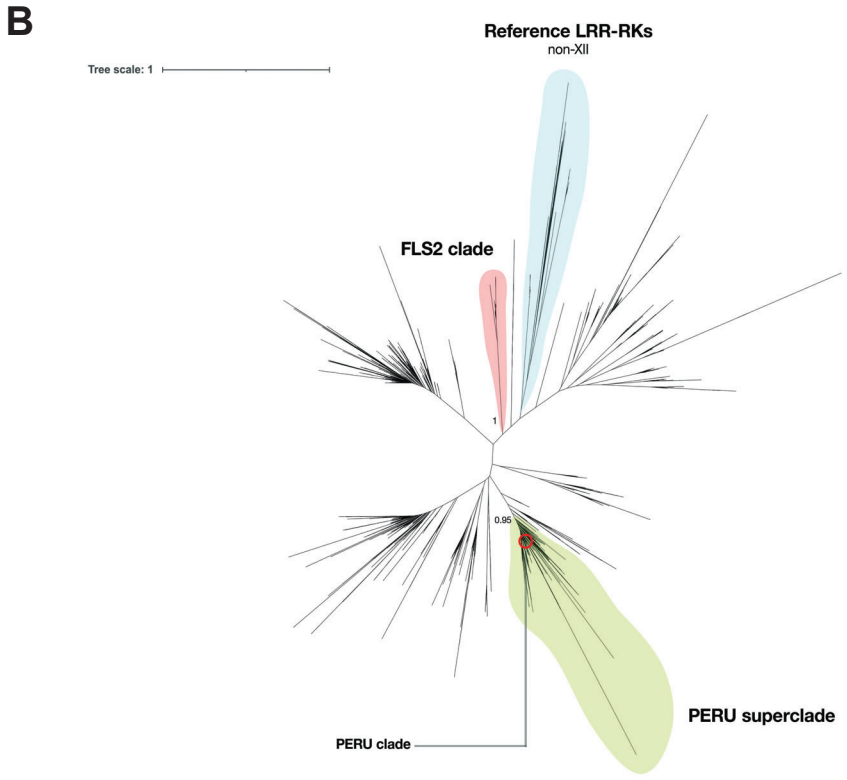
B
Tree scale: 1
Reference LRR-RKs
non-XII
FLS2 clade
1
0.95
PERU clade
PERU superclade

Fig S9. PERU and FLS2 formed distinct, well-supported clades within the LRR-RK subgroup XII. A. A phylogenetic tree showing the LRR-RK classification for 42,697 LRR-RK proteins. Both PERU and FLS2 are located within the XII subgroup and have monophyletic origin. **B.** LRR-RK subgroup XII phylogenetic tree showing PERU and FLS2 are located in distinct and well-supported phylogenetic clades. The numerical values presented correspond to the bootstrap values for major branches for the clades that contain PERU and FLS2.

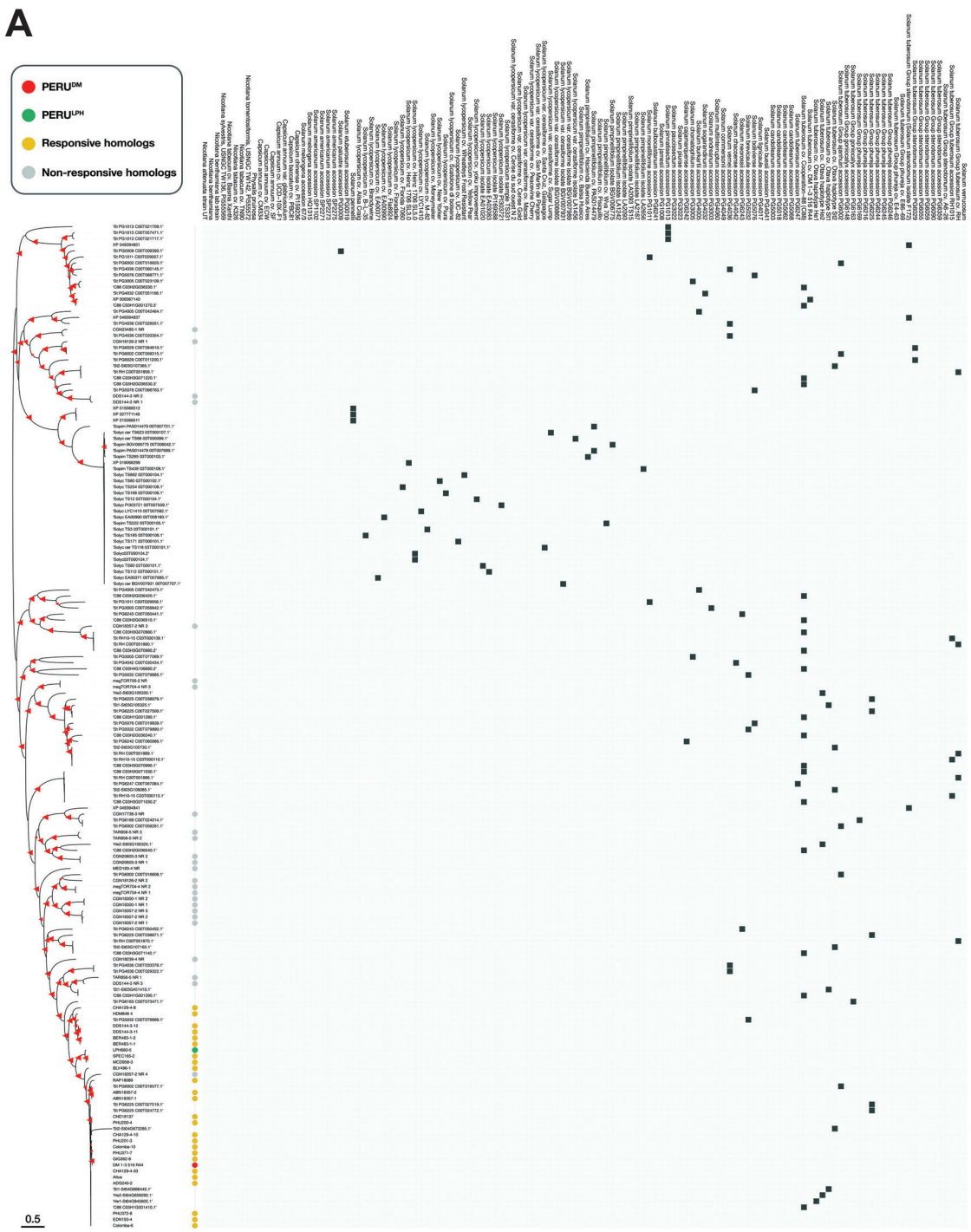
A
PERU^DM
PERU^LPH
Responsive homologs
Non-responsive homologs
0.5

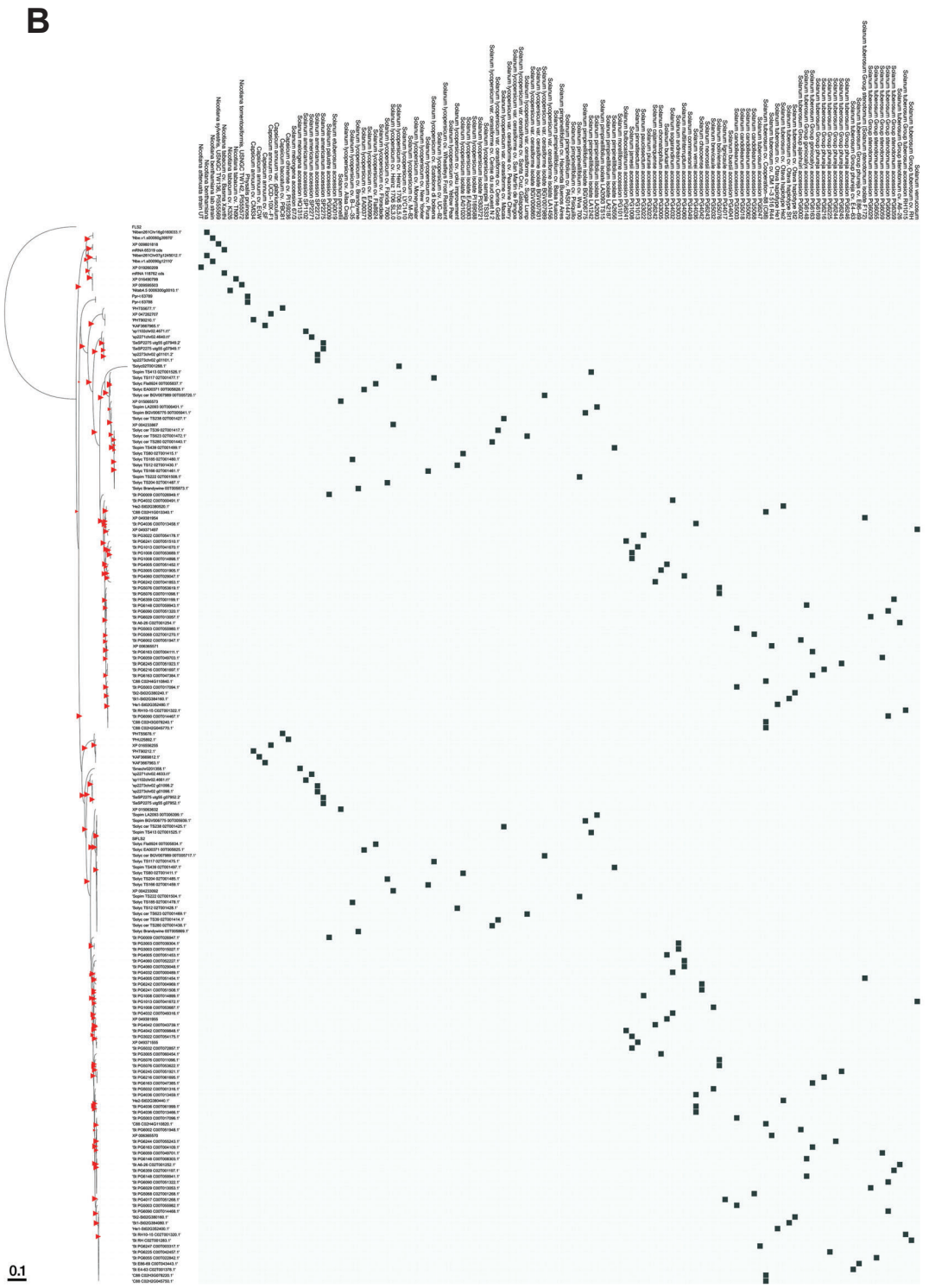
B
0.1

Fig S10. Heatmap representation of presence/absence of PERU phylogenetic clade across *Solanum* species. **A.** The $PERU^{DM}$, $PERU^{LPH}$, and the Pep-13 responsive homologs clustered together in a single clade, while the non-responsive homologs were scattered throughout the phylogenetic tree. **B.** FLS2 clade demonstrated uniformity in distribution and little variation across the Solanum genus, with most species possessing at least one copy. The bootstrap values for all branches are illustrated with triangles.

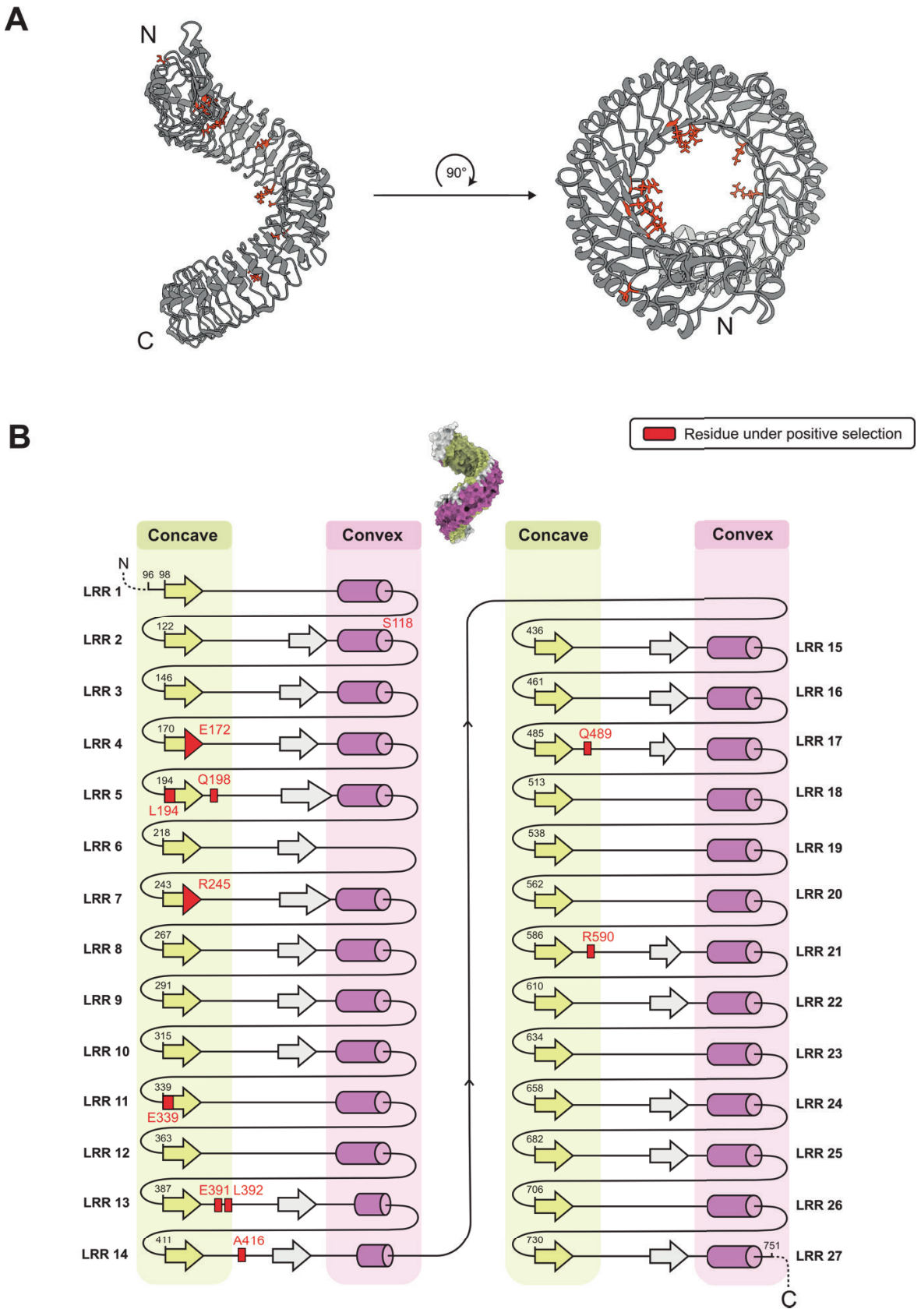
A
N
C
90°
N
B
Residue under positive selection
Concave
Convex
Concave
Convex
N
96 98
LRR 1
122
S118
LRR 2
146
LRR 3
170
E172
LRR 4
194
Q198
LRR 5
L194
218
LRR 6
243
R245
LRR 7
267
LRR 8
291
LRR 9
315
LRR 10
339
LRR 11
E339
363
LRR 12
387
E391 L392
LRR 13
411
A416
LRR 14
436
LRR 15
461
LRR 16
485
Q489
LRR 17
513
LRR 18
538
LRR 19
562
LRR 20
586
R590
LRR 21
610
LRR 22
634
LRR 23
658
LRR 24
682
LRR 25
706
LRR 26
730
751
LRR 27
C

Fig S11. AlphaFold2 model of PERU^{DM}-ectodomain with residues found under positive selection. **A**. AlphaFold2 model for the ectodomain of PERU^{DM}, which closely resembles the experimentally validated structure of FLS2. The 11 residues found to be under positive selection after performing PAML analysis are marked in red. **B.** Schematic representation of the LRR domain of PERU^{DM} (residues 96-751) including secondary structures and the residues highlighted in (A).

Table S1. Diversifying selection analysis using PAML. CODELM from the PAML software was used, six models were tested (Null models M0, M1, M7 and alternative models M2, M3, M8).

Model of selection	lnL[a]	Estimates of parameters	Positively selected sites[b]	Model comparison	2ΔL[c]	d.f[d]	p-value
M0 (one-ratio)	-7990.55	ω=0.547	Not allowed				
M1 (nearly neutral)	-7864.81	p_0=0.702	Not allowed				
M2 (positive selection)	-7805.74	p_0=0.676, p_1=0.280, p_2=0.044, ω_2=6.959	**118 S**, 172 E, 194 L, **198 Q**, **245 R**, **339 E**, **391 E**, **392 L**, **416 A**, **489 Q**, **590 R**	M1 vs. M2	118.14	2	0.0
M3 (discrete)	-7799,84	p_0=0.760, p_1=0.225, p_2=0.015, ω_0=0.008 ω_1=2.032 ω_2=12.91	**4 A,** 5 F, 6 T**, 7 F,** 12 I**, 16 L,** 22 Q, 26 T, 31 A, 46 Y**, 48 N,** 52 S**, 54 A, 56 N, 59 R,** 63 V, 65 C**,** 66 G, 67 S**, 68 R, 71 R, 79 D, 81 T,** 85 T, 90 L, 99 L**,** 102 G, **103 S,** 115 A, **116 R, 118 S,** 119 R**, 124 D, 127 F, 129 K,** 130 F, 131 R**, 142 E, 143 R, 145 Q, 146 V, 150 R, 151 S,157 F, 172 E**, 180 G**, 193 N, 194 L, 196 S, 197 I, 198 Q, 199 H , 201 K, 215 S,** 217 E, 218 V**,** 223 N**, 225 S**, 241 L, 243 E**, 245 R, 248 V, 252 H, 257 K, 267 K, 272 G,** 291 I**, 296 A, 315 K, 317 A, 325 S, 339 E, 344 K,** 348 K, 382 L**,** 387 E, 388 L**, 389 N, 390 L, 391 E, 392 L, 411 I, 412 M, 413 S, 416 A, 472 L, 479 Y, 484 H, 485 Y, 489 Q, 510 N, 512 T, 513 S**, 515 Y**, 534 K, 562 D, 564 D,** 566 S**,** 579 H**, 581 M**, 587 L**, 588 D, 590 R,** 591 N, 607 H**, 621 A, 629 I, 634 F, 635 L, 636 H, , 658 K, 660 H, 676 G,** 681 V**,** 693 S,697 S, 698 V, 702 V, 703 G, 705 E, 706 F**, 713 D,** 714 I**, 717 S, 722 M,** 727 N, 738 L, 745 G, 749 K**, 758 D,** 764 G**, 765 S,** 774 A, 778 K**, 785 K, 788 V,** 791 L, 792 V, **803 T, 805 V,820 R,** 825 S, 827 A, 844 L, 845 G**, 862 V, 864 R,** 893 R, 901 V, 926 D, 927 K, 961 S, 1000 Y, **1059 L,** 1066 V, **1078 R**, 1079 L, 1087 A, **1098 A,** 1102 T, **1118 K**, 1123 A	M0 vs. M3	381.42	4	0.0
M7 (beta)	-7872.88	p=0.006, q=0.009	Not allowed				
M8 (beta&ω)	-7808.25	p_0=0.937, p=0.025, q=0.066, ω_1=5.70	**118 S**, 142 E, 172 E, 194 L, **198 Q**, **245 R**, **339 E**, **391 E**, **392 L**, 416 A, **489 Q**, 590 R	M7 vs. M8	129.26	2	0.0

[a]lnL = log likelihood value.

[b]Amino acid sites inferred to be under diversifying selection with a probability >95% are shown, >99% are shown in bold, sites predicted by the three models are underlined.

[c]Likelihood ratio test: 2ΔL= 2(lnL alternative hypothesis - lnL null hypothesis).

Table S2. Sequence of primers used in this study.

Primer name	Sequence
PCR_AP1-fw	ATGACCAAATATCCGCCTTT
PCR_AP1-rv	CCAAGGTACATTTGCCAAAG
PCR_AP2-fw	CACCCCTTACCACTTTTCTT
PCR_AP2-rv	ATAAAGCATTGGGTCGAACT
PCR_AP3-fw	GTGTTATTTGAGTTGCAGG
PCR_AP3-rv	AGAAGTGGTGGCATTTGG
PCR_AP4-fw	AGGAGGGGAAAAGATATCGA
PCR_AP4-rv	CAAGGACGGGAACTTTCTTA
PCR_AP5-fw	ATGTCACTAGCCTAGAATTT
PCR_AP5-rv	GTGCTTTATCTAACAACGTA
PCR_AP6-fw	GGATCTTCTTGAAGGCATTG
PCR_AP6-rv	TTTTGGATGATCTGGCACG
PCR_AP7-fw	TATACAACTGACCCCTACTT
PCR_AP7-rv	TCCCCACAACTAGTACTATT
PCR_AP8-fw	AGCCTTGGAGCAACGGTAAA
PCR_AP8-rv	GGCTCGTTTGGTGTGAGAGA
HRM-1-fw	AATTTGTGTTTTGGGCTTCC
HRM-1-rv	AACGCTAGAGGAAGAATGTT
HRM-2-fw	GACCACAAACAGTAGACAGT
HRM-2-rv	AAACTCCGTTCCAAGTCAAA
HRM-3-fw	GTGAAACATAGCACTGCTAGA
HRM-3-rv	CACTAGGATGATGGTCTTTGA
HRM-4-fw	ACTCAGTCGTCAGTAAAAGT
HRM-4-rv	CATGATGGGTACAATGTAT
HRM-5-fw	ATACGATATGTATGCATCCT
HRM-5-rv	CCAAACTTTTAGTAGTAACG
HRM-6-fw	GAGTTCCAATATACCAACAG
HRM-6-rv	CATATATGTCACAGCCTTTA
HRM-7-fw	CATAAAGCTGTAATATGTGC
HRM-7-rv	AGTTCCATCAAGTAGCTATC
HRM-8-fw	CAAGAGACTTACAACATGTG
HRM-8-rv	GTATTCTGATCCAAATGG
HRM-9-fw	AGCTTATCTGTTTTTCTAGC
HRM-9-rv	CTCTACTCTGTATGGTCCAC

HRM-10-fw	GACCACAAACAGTAGACAGT
HRM-10-rv	AAACTCCGTTCCAAGTCAAA
HRM-11-fw	ACACTTCACCATTACACTTC
HRM-11-rv	CACAGAAACTATACAGAAGACA
HRM-12-fw	CTAAGCTTATCAATTACGAG
HRM-12-rv	ACGTGGTAAAACTGATAA
HRM-13-fw	AATTCTAGCTCCGCCACTGG
HRM-13-rv	GGTTACGGAGAAGGGTTGCA
CAPS1-fw	GCTTGTCTCTGTGTTATTGC
CAPS1-rv	ACTAGGAGAAGCAGTAGGAG
CAPS2-fw	TGCTTTAGTTTGATCGGTGA
CAPS2-rv	TGGAGAGAGAGTTCAGTAGG
CAPS3-fw	CTTAGTCTCTGCCTGATGTC
CAPS3-rv	AAAGGCTGCGATACTGATAG
CAPS4-fw	GCTATCCTACAAAGACCGTC
CAPS4-rv	GCAAATAAACTCTCAAAGGGA
a-start-fw	CACCATGGAGAAGGCCTTGAGAT
a-stop-rv	CTAATTACTTTGAGCCGAGGT
b-start-fw	CACCATGGAGAAAGCCTTCACAT
b-stop-rv	TCAGCATGCAAGAAGTTG
b-start-fw2	CACCCACATGTTACTAGCGATATC
b-start-fw3	CACCACATGTTACTAGCGATATCA
c-start-fw	CACCATGATGGAGAAAACAGAGG
c-stop-rv	CTGGATCACGCTGCCTCG
sgRNA-1-fw	ATTGAGAAATAGCACGCTTGTCT
sgRNA-2-fw	ATTGGTGCCTGTAAGAGTCATGT
sgRNA-3-fw	ATTGAGTGAAACTTCTTGCAATG
sgRNA-4-fw	ATTGAATTTGATGAAGTTAGCCG
sgRNA-1-rv	AAACAGACAAGCGTGCTATTTCT
sgRNA-2-rv	AAACACATGACTCTTACAGGCAC
sgRNA-3-rv	AAACCATTGCAAGAAGTTTCACT
sgRNA-4-rv	AAACCGGCTAACTTCATCAAATT
CC-238-fw	TGCAGCGTCTCTTCCTCGAT
CC-1440-rv	GATGACCACACACGTGTCCT
CC-4225-fw	TTGATGAAGTTAGCCGTGGAGA
CC-5129-rv	TTTCTCAAGTCCAGGCGCTG

Data S1. Pep-25 and the three peptide mutants were tested for HR induction on 477 genotypes. HR was scored from 0 to 1, and only genotypes with HR value higher than. 0.2 were considered for further analysis. [a] Unique ID for Centre for Genetic Resources, the Netherlands (CGN) (https://cgngenis.wur.nl/), and SolR gene database (https://www.plantbreeding.wur.nl/SolRgenes/). [b] Species name (Spooner et al. 2014). [c] Cladistic relationships are based on plastid or nuclear investigations (Spooner et al. 2014).

Data S2. Genome metadata used in the phylogenomic analysis.

Data S3. Per species statistics of LRR-RK distribution.

Data S4. Per genome statistics of LRR-RK distribution.

Data S5. PERU clade sequence and metadata.

Data S6. List of responsive and non-responsive homologs sequence and metadata.

Data S7. Reference LRR-RK sequence and metadata.

Data S8. LRR-RK sequence and metadata.

Data S9. LRR-RK Subgroup XII sequence and metadata.

Data S10. FLS2 clade sequence and metadata.

References and Notes

1. B. P. M. Ngou, H.-K. Ahn, P. Ding, J. D. G. Jones, Mutual potentiation of plant immunity by cell-surface and intracellular receptors. *Nature* **592**, 110–115 (2021). doi:10.1038/s41586-021-03315-7 Medline

2. M. Yuan, Z. Jiang, G. Bi, K. Nomura, M. Liu, Y. Wang, B. Cai, J.-M. Zhou, S. Y. He, X.-F. Xin, Pattern-recognition receptors are required for NLR-mediated plant immunity. *Nature* **592**, 105–109 (2021). doi:10.1038/s41586-021-03316-6 Medline

3. J. Rhodes, C. Zipfel, J. D. G. Jones, B. P. M. Ngou, Concerted actions of PRR- and NLR-mediated immunity. *Essays Biochem.* **66**, 501–511 (2022). doi:10.1042/EBC20220067 Medline.

4. R. N. Pruitt, F. Locci, F. Wanke, L. Zhang, S. C. Saile, A. Joe, D. Karelina, C. Hua, K. Fröhlich, W.-L. Wan, M. Hu, S. Rao, S. C. Stolze, A. Harzen, A. A. Gust, K. Harter, M. H. A. J. Joosten, B. P. H. J. Thomma, J.-M. Zhou, J. L. Dangl, D. Weigel, H. Nakagami, C. Oecking, F. E. Kasmi, J. E. Parker, T. Nürnberger, The EDS1-PAD4-ADR1 node mediates *Arabidopsis* pattern-triggered immunity. *Nature* **598**, 495–499 (2021). doi:10.1038/s41586-021-03829-0 Medline

5. B. P. M. Ngou, R. Heal, M. Wyler, M. W. Schmid, J. D. G. Jones, Concerted expansion and contraction of immune receptor gene repertoires in plant genomes. *Nat. Plants* **8**, 1146–1152 (2022). doi:10.1038/s41477-022-01260-5 Medline

6. C. Aguilera-Galvez, N. Champouret, H. Rietman, X. Lin, D. Wouters, Z. Chu, J. D. G. Jones, J. H. Vossen, R. G. F. Visser, P. J. Wolters, V. G. A. A. Vleeshouwers, Two different *R* gene loci co-evolved with *Avr2* of *Phytophthora infestans* and confer distinct resistance specificities in potato. *Stud. Mycol.* **89**, 105–115 (2018). doi:10.1016/j.simyco.2018.01.002 Medline

7. T. Nürnberger, D. Nennstiel, T. Jabs, W. R. Sacks, K. Hahlbrock, D. Scheel, High affinity binding of a fungal oligopeptide elicitor to parsley plasma membranes triggers multiple defense responses. *Cell* **78**, 449–460 (1994). doi:10.1016/0092-8674(94)90423-5 Medline

8. T. Nürnberger, D. Nennstiel, K. Hahlbrock, D. Scheel, Covalent cross-linking of the *Phytophthora megasperma* oligopeptide elicitor to its receptor in parsley membranes. *Proc. Natl. Acad. Sci. U.S.A.* **92**, 2338–2342 (1995). doi:10.1073/pnas.92.6.2338 Medline

9. V. G. A. A. Vleeshouwers, S. Raffaele, J. H. Vossen, N. Champouret, R. Oliva, M. E. Segretin, H. Rietman, L. M. Cano, A. Lokossou, G. Kessel, M. A. Pel, S. Kamoun, Understanding and exploiting late blight resistance in the age of effectors. *Annu. Rev. Phytopathol.* **49**, 507–531 (2011). doi:10.1146/annurev-phyto-072910-095326 Medline

10. F. Brunner, S. Rosahl, J. Lee, J. J. Rudd, C. Geiler, S. Kauppinen, G. Rasmussen, D. Scheel, T. Nürnberger, Pep-13, a plant defense-inducing pathogen-associated pattern from *Phytophthora* transglutaminases. *EMBO J.* **21**, 6681–6688 (2002). doi:10.1093/emboj/cdf667 Medline

11. B. J. Haas, S. Kamoun, M. C. Zody, R. H. Y. Jiang, R. E. Handsaker, L. M. Cano, M. Grabherr, C. D. Kodira, S. Raffaele, T. Torto-Alalibo, T. O. Bozkurt, A. M. V. Ah-Fong, L. Alvarado, V. L. Anderson, M. R. Armstrong, A. Avrova, L. Baxter, J. Beynon, P. C.

Boevink, S. R. Bollmann, J. I. B. Bos, V. Bulone, G. Cai, C. Cakir, J. C. Carrington, M. Chawner, L. Conti, S. Costanzo, R. Ewan, N. Fahlgren, M. A. Fischbach, J. Fugelstad, E. M. Gilroy, S. Gnerre, P. J. Green, L. J. Grenville-Briggs, J. Griffith, N. J. Grünwald, K. Horn, N. R. Horner, C.-H. Hu, E. Huitema, D.-H. Jeong, A. M. E. Jones, J. D. G. Jones, R. W. Jones, E. K. Karlsson, S. G. Kunjeti, K. Lamour, Z. Liu, L. Ma, D. Maclean, M. C. Chibucos, H. McDonald, J. McWalters, H. J. G. Meijer, W. Morgan, P. F. Morris, C. A. Munro, K. O'Neill, M. Ospina-Giraldo, A. Pinzón, L. Pritchard, B. Ramsahoye, Q. Ren, S. Restrepo, S. Roy, A. Sadanandom, A. Savidor, S. Schornack, D. C. Schwartz, U. D. Schumann, B. Schwessinger, L. Seyer, T. Sharpe, C. Silvar, J. Song, D. J. Studholme, S. Sykes, M. Thines, P. J. I. van de Vondervoort, V. Phuntumart, S. Wawra, R. Weide, J. Win, C. Young, S. Zhou, W. Fry, B. C. Meyers, P. van West, J. Ristaino, F. Govers, P. R. J. Birch, S. C. Whisson, H. S. Judelson, C. Nusbaum, Genome sequence and analysis of the Irish potato famine pathogen *Phytophthora infestans*. *Nature* **461**, 393–398 (2009). doi:10.1038/nature08358 Medline

12. W. E. Fry, P. R. J. Birch, H. S. Judelson, N. J. Grünwald, G. Danies, K. L. Everts, A. J. Gevens, B. K. Gugino, D. A. Johnson, S. B. Johnson, M. T. McGrath, K. L. Myers, J. B. Ristaino, P. D. Roberts, G. Secor, C. D. Smart, Five reasons to consider *Phytophthora infestans* a reemerging pathogen. *Phytopathology* **105**, 966–981 (2015). doi:10.1094/PHYTO-01-15-0005-FI Medline

13. X. Lin, Y. C. Torres Ascurra, H. Fillianti, L. Dethier, L. de Rond, E. Domazakis, C. Aguilera-Galvez, A. Y. Kiros, E. Jacobsen, R. G. F. Visser, T. Nürnberger, V. G. A. A. Vleeshouwers, Recognition of Pep-13/25 MAMPs of *Phytophthora* localizes to an *RLK* locus in *Solanum microdontum*. *Front. Plant Sci.* **13**, 1037030 (2023). doi:10.3389/fpls.2022.1037030 Medline

14. G. M. Pham, J. P. Hamilton, J. C. Wood, J. T. Burke, H. Zhao, B. Vaillancourt, S. Ou, J. Jiang, C. R. Buell, Construction of a chromosome-scale long-read reference genome assembly for potato. *Gigascience* **9**, giaa100 (2020). doi:10.1093/gigascience/giaa100 Medline

15. V. G. A. A. Vleeshouwers, R. Finkers, D. Budding, M. Visser, M. M. J. Jacobs, R. van Berloo, M. Pel, N. Champouret, E. Bakker, P. Krenek, H. Rietman, D. Huigen, R. Hoekstra, A. Goverse, B. Vosman, E. Jacobsen, R. G. F. Visser, Sol*R*gene: An online database to explore disease resistance genes in tuber-bearing *Solanum* species. *BMC Plant Biol.* **11**, 116 (2011). doi:10.1186/1471-2229-11-116 Medline

16. F. Boutrot, C. Zipfel, Function, discovery, and exploitation of plant pattern recognition receptors for broad-spectrum disease resistance. *Annu. Rev. Phytopathol.* **55**, 257–286 (2017). doi:10.1146/annurev-phyto-080614-120106 Medline

17. W.-L. Wan, K. Fröhlich, R. N. Pruitt, T. Nürnberger, L. Zhang, Plant cell surface immune receptor complex signaling. *Curr. Opin. Plant Biol.* **50**, 18–28 (2019). doi:10.1016/j.pbi.2019.02.001 Medline

18. A. M. Escocard de Azevedo Manhães, F. A. Ortiz-Morea, P. He, L. Shan, Plant plasma membrane-resident receptors: Surveillance for infections and coordination for growth and development. *J. Integr. Plant Biol.* **63**, 79–101 (2021). doi:10.1111/jipb.13051 Medline

19. D. Couto, C. Zipfel, Regulation of pattern recognition receptor signalling in plants. *Nat. Rev. Immunol.* **16**, 537–552 (2016). doi:10.1038/nri.2016.77 Medline

20. T. A. DeFalco, C. Zipfel, Molecular mechanisms of early plant pattern-triggered immune signaling. *Mol. Cell* **81**, 3449–3467 (2021). doi:10.1016/j.molcel.2021.07.029 Medline

21. J. Du, E. Verzaux, A. Chaparro-Garcia, G. Bijsterbosch, L. C. P. Keizer, J. Zhou, T. W. H. Liebrand, C. Xie, F. Govers, S. Robatzek, E. A. G. van der Vossen, E. Jacobsen, R. G. F. Visser, S. Kamoun, V. G. A. A. Vleeshouwers, Elicitin recognition confers enhanced resistance to *Phytophthora infestans* in potato. *Nat. Plants* **1**, 15034 (2015). doi:10.1038/nplants.2015.34 Medline

22. S. H. E. J. Gabriëls, J. H. Vossen, S. K. Ekengren, G. van Ooijen, A. M. Abd-El-Haliem, G. C. van den Berg, D. Y. Rainey, G. B. Martin, F. L. W. Takken, P. J. de Wit, M. H. A. J. Joosten, An NB-LRR protein required for HR signalling mediated by both extra- and intracellular resistance proteins. *Plant J.* **50**, 14–28 (2007). doi:10.1111/j.1365-313X.2007.03027.x Medline

23. C.-H. Wu, K. Belhaj, T. O. Bozkurt, M. S. Birk, S. Kamoun, Helper NLR proteins NRC2a/b and NRC3 but not NRC1 are required for Pto-mediated cell death and resistance in *Nicotiana benthamiana*. *New Phytol.* **209**, 1344–1352 (2016). doi:10.1111/nph.13764 Medline

24. J. Kourelis, M. P. Contreras, A. Harant, H. Pai, D. Lüdke, H. Adachi, L. Derevnina, C.-H. Wu, S. Kamoun, The helper NLR immune protein NRC3 mediates the hypersensitive cell death caused by the cell-surface receptor Cf-4. *PLOS Genet.* **18**, e1010414 (2022). doi:10.1371/journal.pgen.1010414 Medline

25. J. Ordon, J. Gantner, J. Kemna, L. Schwalgun, M. Reschke, J. Streubel, J. Boch, J. Stuttmann, Generation of chromosomal deletions in dicotyledonous plants employing a user-friendly genome editing toolkit. *Plant J.* **89**, 155–168 (2017). doi:10.1111/tpj.13319 Medline

26. J. Gantner, J. Ordon, C. Kretschmer, R. Guerois, J. Stuttmann, An EDS1-SAG101 Complex is essential for TNL-mediated immunity in *Nicotiana benthamiana*. *Plant Cell* **31**, 2456–2474 (2019). doi:10.1105/tpc.19.00099 Medline

27. V. G. A. A. Vleeshouwers, W. van Dooijeweert, L. C. Paul Keizer, L. Sijpkes, F. Govers, L. T. Colon, A Laboratory assay for *Phytophthora infestans* resistance in various *Solanum* species reflects the field situation. *Eur. J. Plant Pathol.* **105**, 241–250 (1999). doi:10.1023/A:1008710700363

28. S. Lacombe, A. Rougon-Cardoso, E. Sherwood, N. Peeters, D. Dahlbeck, H. P. van Esse, M. Smoker, G. Rallapalli, B. P. H. J. Thomma, B. Staskawicz, J. D. G. Jones, C. Zipfel, Interfamily transfer of a plant pattern-recognition receptor confers broad-spectrum bacterial resistance. *Nat. Biotechnol.* **28**, 365–369 (2010). doi:10.1038/nbt.1613 Medline

29. I. Albert, H. Böhm, M. Albert, C. E. Feiler, J. Imkampe, N. Wallmeroth, C. Brancato, T. M. Raaymakers, S. Oome, H. Zhang, E. Krol, C. Grefen, A. A. Gust, J. Chai, R. Hedrich, G. Van den Ackerveken, T. Nürnberger, An RLP23-SOBIR1-BAK1 complex mediates NLP-triggered immunity. *Nat. Plants* **1**, 15140 (2015). doi:10.1038/nplants.2015.140 Medline

30. D. M. Spooner, M. Ghislain, R. Simon, S. H. Jansky, T. Gavrilenko, Systematics, diversity, genetics, and evolution of wild and cultivated potatoes. *Bot. Rev.* **80**, 283–383 (2014). doi:10.1007/s12229-014-9146-y

31. B. P. M. Ngou, P. Ding, J. D. G. Jones, Thirty years of resistance: Zig-zag through the plant immune system. *Plant Cell* **34**, 1447–1478 (2022). doi:10.1093/plcell/koac041 Medline

32. L. Quintana-Murci, A. G. Clark, Population genetic tools for dissecting innate immunity in humans. *Nat. Rev. Immunol.* **13**, 280–293 (2013). doi:10.1038/nri3421 Medline

33. P. S. Kahlon, R. Stam, Polymorphisms in plants to restrict losses to pathogens: From gene family expansions to complex network evolution. *Curr. Opin. Plant Biol.* **62**, 102040 (2021). doi:10.1016/j.pbi.2021.102040 Medline

34. Z. Yang, PAML 4: Phylogenetic analysis by maximum likelihood. *Mol. Biol. Evol.* **24**, 1586–1591 (2007). doi:10.1093/molbev/msm088 Medline

35. Z. Liu, J. I. B. Bos, M. Armstrong, S. C. Whisson, L. da Cunha, T. Torto-Alalibo, J. Win, A. O. Avrova, F. Wright, P. R. J. Birch, S. Kamoun, Patterns of diversifying selection in the phytotoxin-like scr74 gene family of *Phytophthora infestans*. *Mol. Biol. Evol.* **22**, 659–672 (2005). doi:10.1093/molbev/msi049 Medline

36. Y. Sun, L. Li, A. P. Macho, Z. Han, Z. Hu, C. Zipfel, J.-M. Zhou, J. Chai, Structural basis for flg22-induced activation of the *Arabidopsis* FLS2-BAK1 immune complex. *Science* **342**, 624–628 (2013). doi:10.1126/science.1243825 Medline

37. P. Buscaill, R. A. L. van der Hoorn, Defeated by the nines: Nine extracellular strategies to avoid microbe-associated molecular patterns recognition in plants. *Plant Cell* **33**, 2116–2130 (2021). doi:10.1093/plcell/koab109 Medline

38. Y. Wang, R. N. Pruitt, T. Nürnberger, Y. Wang, Evasion of plant immunity by microbial pathogens. *Nat. Rev. Microbiol.* **20**, 449–464 (2022). doi:10.1038/s41579-022-00710-3 Medline

39. N. R. Colaianni, K. Parys, H.-S. Lee, J. M. Conway, N. H. Kim, N. Edelbacher, T. S. Mucyn, M. Madalinski, T. F. Law, C. D. Jones, Y. Belkhadir, J. L. Dangl, A complex immune response to flagellin epitope variation in commensal communities. *Cell Host Microbe* **29**, 635–649.e9 (2021). doi:10.1016/j.chom.2021.02.006 Medline

40. U. Fürst, Y. Zeng, M. Albert, A. K. Witte, J. Fliegmann, G. Felix, Perception of Agrobacterium tumefaciens flagellin by FLS2^{XL} confers resistance to crown gall disease. *Nat. Plants* **6**, 22–27 (2020). doi:10.1038/s41477-019-0578-6 Medline

41. K. Parys, N. R. Colaianni, H.-S. Lee, U. Hohmann, N. Edelbacher, A. Trgovcevic, Z. Blahovska, D. Lee, A. Mechtler, Z. Muhari-Portik, M. Madalinski, N. Schandry, I. Rodríguez-Arévalo, C. Becker, E. Sonnleitner, A. Korte, U. Bläsi, N. Geldner, M. Hothorn, C. D. Jones, J. L. Dangl, Y. Belkhadir, Signatures of antagonistic pleiotropy in a bacterial flagellin epitope. *Cell Host Microbe* **29**, 620–634.e9 (2021). doi:10.1016/j.chom.2021.02.008 Medline

42. S. Snoeck, B. W. Abramson, A. G. K. Garcia, A. N. Egan, T. P. Michael, A. D. Steinbrenner, Evolutionary gain and loss of a plant pattern-recognition receptor for HAMP recognition. *eLife* **11**, e81050 (2022). doi:10.7554/eLife.81050 Medline

43. Y. Wei, A. Balaceanu, J. S. Rufian, C. Segonzac, A. Zhao, R. J. L. Morcillo, A. P. Macho, An immune receptor complex evolved in soybean to perceive a polymorphic bacterial flagellin. *Nat. Commun.* **11**, 3763 (2020). doi:10.1038/s41467-020-17573-y Medline

44. T. Murakami, Y. Katsuragi, H. Hirai, K. Wataya, M. Kondo, F.-S. Che, Distribution of flagellin CD2-1, flg22, and flgII-28 recognition systems in plant species and regulation of plant immune responses through these recognition systems. *Biosci. Biotechnol. Biochem.* **86**, 490–501 (2022). doi:10.1093/bbb/zbac007 Medline

45. L. Zhang, C. Hua, R. N. Pruitt, S. Qin, L. Wang, I. Albert, M. Albert, J. A. L. van Kan, T. Nürnberger, Distinct immune sensor systems for fungal endopolygalacturonases in closely related Brassicaceae. *Nat. Plants* **7**, 1254–1263 (2021). doi:10.1038/s41477-021-00982-2 Medline

46. A. Thogani, Git Repository: Phylogenetics of PERU and FLS2 LRR-RK immune receptors in the Solanaceae plant family, version 1, Zenodo (2023); https://doi.org/10.5281/zenodo.8079625.

47. S. Landeo Villanueva, M. C. Malvestiti, W. van Ieperen, M. H. A. J. Joosten, J. A. L. van Kan, Red light imaging for programmed cell death visualization and quantification in plant-pathogen interactions. *Mol. Plant Pathol.* **22**, 361–372 (2021). doi:10.1111/mpp.13027 Medline

48. D. Tang, Y. Jia, J. Zhang, H. Li, L. Cheng, P. Wang, Z. Bao, Z. Liu, S. Feng, X. Zhu, D. Li, G. Zhu, H. Wang, Y. Zhou, Y. Zhou, G. J. Bryan, C. R. Buell, C. Zhang, S. Huang, Genome evolution and diversity of wild and cultivated potatoes. *Nature* **606**, 535–541 (2022). doi:10.1038/s41586-022-04822-x Medline

49. T. Murashige, F. Skoog, A revised medium for rapid growth and bio assays with tobacco tissue cultures. *Physiol. Plant.* **15**, 473–497 (1962). doi:10.1111/j.1399-3054.1962.tb08052.x

50. E. Domazakis, D. Wouters, R. G. F. Visser, S. Kamoun, M. H. A. J. Joosten, V. G. A. A. Vleeshouwers, The ELR-SOBIR1 complex functions as a two-component receptor-like kinase to mount defense against *Phytophthora infestans*. *Mol. Plant Microbe Interact.* **31**, 795–802 (2018). doi:10.1094/MPMI-09-17-0217-R Medline

51. J. Du, H. Rietman, V. G. A. A. Vleeshouwers, W. T. Luo, Agroinfiltration and PVX agroinfection in potato and *Nicotiana benthamiana*. *J. Vis. Exp.* **83**, e50971 (2014). Medline

52. Y. Torres Ascurra, X. Lin, P. J. Wolters, V. G. A. A. Vleeshouwers, in *Solanum tuberosum: Methods and Protocols*, D. Dobnik, K. Gruden, Ž. Ramšak, A. Coll, Eds. (Springer, 2021), pp. 315-330.

53. R. G. F. Visser, in *Plant Tissue Culture Manual: Supplement 7*, K. Lindsey, Ed. (Springer, 1997), pp. 301-309.

54. C. Engler, M. Youles, R. Gruetzner, T.-M. Ehnert, S. Werner, J. D. G. Jones, N. J. Patron, S. Marillonnet, A golden gate modular cloning toolbox for plants. *ACS Synth. Biol.* **3**, 839–843 (2014). doi:10.1021/sb4001504 Medline

55. D. Monino-Lopez, M. Nijenhuis, L. Kodde, S. Kamoun, H. Salehian, K. Schentsnyi, R. Stam, A. Lokossou, A. Abd-El-Haliem, R. G. F. Visser, J. H. Vossen, Allelic variants of the NLR protein Rpi-chc1 differentially recognize members of the *Phytophthora infestans* PexRD12/31 effector superfamily through the leucine-rich repeat domain. *Plant J.* **107**, 182–197 (2021). doi:10.1111/tpj.15284 Medline

56. S. Landeo Villanueva, M. C. Malvestiti, W. van Ieperen, M. H. A. J. Joosten, J. A. L. van Kan, Red light imaging for programmed cell death visualization and quantification in plant-pathogen interactions. *Mol. Plant Pathol.* **22**, 361–372 (2021). doi:10.1111/mpp.13027 Medline

57. M. A. Pombo, R. N. Ramos, Y. Zheng, Z. Fei, G. B. Martin, H. G. Rosli, Transcriptome-based identification and validation of reference genes for plant-bacteria interaction studies using *Nicotiana benthamiana*. *Sci. Rep.* **9**, 1632 (2019). doi:10.1038/s41598-018-38247-2 Medline

58. C. E. Caten, J. L. Jinks, Spontaneous variability of single isolates of *Phytophthora infestans*. I. Cultural variation. *Can. J. Bot.* **46**, 329–348 (1968). doi:10.1139/b68-055

59. S. R. Eddy, Accelerated profile HMM searches. *PLOS Comput. Biol.* **7**, e1002195 (2011). doi:10.1371/journal.pcbi.1002195 Medline

60. K. Katoh, D. M. Standley, MAFFT multiple sequence alignment software version 7: Improvements in performance and usability. *Mol. Biol. Evol.* **30**, 772–780 (2013). doi:10.1093/molbev/mst010 Medline

61. M. N. Price, P. S. Dehal, A. P. Arkin, FastTree 2—Approximately maximum-likelihood trees for large alignments. *PLOS ONE* **5**, e9490 (2010). doi:10.1371/journal.pone.0009490 Medline

62. F. Teufel, J. J. Almagro Armenteros, A. R. Johansen, M. H. Gíslason, S. I. Pihl, K. D. Tsirigos, O. Winther, S. Brunak, G. von Heijne, H. Nielsen, SignalP 6.0 predicts all five types of signal peptides using protein language models. *Nat. Biotechnol.* **40**, 1023–1025 (2022). doi:10.1038/s41587-021-01156-3 Medline

63. I. Letunic, P. Bork, Interactive Tree Of Life (iTOL) v5: An online tool for phylogenetic tree display and annotation. *Nucleic Acids Res.* **49**, W293–W296 (2021). doi:10.1093/nar/gkab301 Medline

64. K. Tamura, G. Stecher, S. Kumar, MEGA11: Molecular evolutionary genetics analysis version 11. *Mol. Biol. Evol.* **38**, 3022–3027 (2021). doi:10.1093/molbev/msab120 Medline

65. Z. Yang, W. S. W. Wong, R. Nielsen, Bayes empirical bayes inference of amino acid sites under positive selection. *Mol. Biol. Evol.* **22**, 1107–1118 (2005). doi:10.1093/molbev/msi097 Medline

66. M. Mirdita, K. Schütze, Y. Moriwaki, L. Heo, S. Ovchinnikov, M. Steinegger, ColabFold: Making protein folding accessible to all. *Nat. Methods* **19**, 679–682 (2022). doi:10.1038/s41592-022-01488-1 Medline

67. J. Jumper, R. Evans, A. Pritzel, T. Green, M. Figurnov, O. Ronneberger, K. Tunyasuvunakool, R. Bates, A. Žídek, A. Potapenko, A. Bridgland, C. Meyer, S. A. A. Kohl, A. J. Ballard, A. Cowie, B. Romera-Paredes, S. Nikolov, R. Jain, J. Adler, T. Back, S. Petersen, D. Reiman, E. Clancy, M. Zielinski, M. Steinegger, M. Pacholska, T. Berghammer, S. Bodenstein, D. Silver, O. Vinyals, A. W. Senior, K. Kavukcuoglu, P. Kohli, D. Hassabis, Highly accurate protein structure prediction with AlphaFold. *Nature* **596**, 583–589 (2021). doi:10.1038/s41586-021-03819-2 Medline